Am J Transl Res 2014;6(4):361-376
www.ajtr.org /ISSN:1943-8141/AJTR0000790

Original Article

S6K1 promotes invasiveness of breast cancer cells in a model of metastasis of triple-negative breast cancer

Yekaterina B Khotskaya[1], Aarthi Goverdhan[1,2], Jia Shen[1,2], Mariano Ponz-Sarvise[1], Shih-Shin Chang[1,2], Ming-Chuan Hsu[1], Yongkun Wei[1], Weiya Xia[1], Dihua Yu[1,2], Mien-Chie Hung[1,2,3,4]

[1]Department of Molecular and Cellular Oncology, The University of Texas MD Anderson Cancer Center, Houston, Texas; [2]The University of Texas Graduate School of Biomedical Sciences at Houston, Houston, Texas; [3]Center for Molecular Medicine and Graduate Institute of Cancer Biology, China Medical University, Taichung 402, Taiwan; [4]Department of Biotechnology, Asia University, Taichung, Taiwan

Received May 10, 2014; Accepted May 15, 2014; Epub July 18, 2014; Published July 30, 2014

Abstract: Breast cancer is the second-leading cause of oncology-related death in US women. Of all invasive breast cancers, patients with tumors lacking expression of the estrogen and progesterone hormone receptors and over-expression of human epidermal growth factor receptor 2 have the poorest clinical prognosis. These referred to as triple-negative breast cancer (TNBC) represent an aggressive form of disease that is marked by early-onset metastasis, high tumor recurrence rate, and low overall survival during the first three years post-diagnosis. In this report, we discuss a novel model of early-onset TNBC metastasis to bone and lungs, derived from MDA-MB-231 cells. Breast cancer cells injected intravenously produced rapid, osteolytic metastases in long bones and spines of athymic nude mice, with concurrent metastasis to lungs, liver, and soft tissues. From the bone metastases, we developed a highly metastatic luciferase-tagged cell line variant named MDA-231-LUC Met. In this report, we demonstrate that the Akt/mTOR/S6K1 axis is hyperactivated in these cells, leading to a dramatic increase in phosphorylation of S6 ribosomal protein at Ser235/236. Lastly, we provide evidence that inhibition of the furthest downstream kinase in the mTOR pathway, S6K1, with a highly specific inhibitor PF-4708671 inhibits cell migration, and thus may provide a potent anti-metastatic adjuvant therapy approach.

Keywords: TNBC, metastasis, bone, S6K1, S6

Introduction

Breast cancer is a group of malignancies that arise in mammary ducts and lobules through acquisition of a series of genetic mutations. It is characterized by an uncontrolled proliferation of malignant cells that over time can degrade the basement membrane, invade neighboring tissues and gain the potential to spread to distant organ sites, such as lungs, liver, brain, and bone. In the clinic, invasive breast cancers are routinely screened for over-expression of human epidermal growth factor receptor 2 (HER2) and expression of estrogen receptor (ER) and progesterone receptor (PR). Therapies are then assigned based on the cancer's molecular profile. Breast cancers that test negative for all three markers are known as the triple-negative breast cancers (TNBC). Together, TNBC represents an aggressive form of the disease that is marked by a high recurrence rate and low overall survival during the first three years post-diagnosis [1-4]. During this time, TNBC patients are frequently diagnosed with metastases to visceral organs or to the bone [3, 5]. Of all metastatic events, bone metastases are the most common [6-8], and brain and bone metastases are the most debilitating [9]. Recent evidence indicates that 44-67% of TNBC patients will develop bone metastasis, versus 43% who develop metastasis to all other non-osseous organs combined [10, 11]. Moreover, since TNBC patients frequently develop therapeutic resistance and rapid disease relapse, metastatic complications pose a great risk for this group of individuals [4].

Bone metastases are clinically difficult to treat in part because they are difficult to model for research purposes [12]. Using syngeneic xeno-

graft models, metastases to multiple organ sites can be achieved. For instance, injection of mouse mammary cancer 4T1, TM40D, or 66c14 cells into the mammary fat pad gives rise to distant metastases in a variety of tissues, such as the brain, liver, lungs, kidneys, and bone [13, 14]. However, concerns exist in the ability of mouse mammary cancer models to mirror the metastatic process in humans. Most human breast cancer cell lines do not metastasize to bone from an orthotopic location, necessitating use of experimental metastasis models. Specifically, to attain bone metastasis, human breast cancer cells are injected into the left ventricle of the heart [15, 16]. Despite its difficulty of execution and high animal mortality rate, intracardiac injection method is still the primary approach used to elucidate mechanisms of bone metastases [17-21]. Compared with intracardiac injections, introduction of breast cancer cells through a lateral tail vein is a less technically challenging model that produces overt lung metastasis [14].

Our current study stems from an observation that parental, genetically unmodified MDA-MB-231 (hereinafter referred to as MDA-231) breast cancer cells [22, 23] are capable of forming a small number of *bona fide* bone metastases when injected intravenously through the lateral tail vein (iv) into athymic nude mice. Using this model, we derived an MDA-231 variant we termed MDA-231-LUC-Met, a luciferase-tagged cell line that is highly metastatic to both bone and lungs when administered intravenously through the tail vein. Importantly, and unlike similar approaches employed previously [18, 19], MDA-231-LUC-Met cells are not single cell clones. Additionally, our model does not enrich for metastases at a single anatomical site, but rather 100% of mice injected with the MDA-231-LUC-Met cell line presented with metastases to lungs, bone, liver, and other organs. Therefore, this cell line can potentially serve as a valuable resource for studying multiple organ metastases including bone metastasis in TNBC, using a simple intravenous method of administration.

To identify signaling pathways that confer MDA-231-LUC-Met cells with increased metastatic potential, we used an unbiased kinase array approach to capture a partial molecular profile of these tumor cells. Using this approach, we detected a dramatic increase in phosphorylation of the ribosomal protein S6 (RPS6), which eventually led us to identify the S6K1 kinase as one of the primary mediators of migration and invasion in MDA-231-LUC-Met cells. S6K1 is best known as the mTORC1 effector kinase that phosphorylates RPS6 at Ser235/236, although it is now known to have several other substrates as well [24]. Phosphorylation of S6K1 at Thr389 by mTOR is a precursor for subsequent phosphorylation at Thr229 by PDK1, resulting in maximal activation of S6K1 [25, 26]. Phosphorylation at the Thr389 site most closely reflects the activated state of S6K1 [27]. In breast cancer, many studies have showed that phosphorylation of S6K1 is a marker of poor patient prognosis, and its knockdown leads to inhibition of proliferation and invasion [28, 29].

In this study, we find that in MDA-231-LUC-Met cells, pharmacological inhibition of S6K1 activity greatly reduced migration and invasion of these cells. In accordance with other studies implicating a role for mTOR and S6K1 in cell motility and metastasis, our study supports the idea that S6K1 is an important regulator of cancer cell migration, invasion, and ultimately metastasis, as an extension of our *in vitro* observations. Hence, targeting S6K1 in an adjuvant setting by small-molecule inhibitors could offer a promising avenue for prevention of distant metastases and improving prognosis for patients with TNBC. Our study lends support to the ongoing effort by pharmaceutical companies to develop S6K1 inhibitors and dual S6K1/Akt inhibitors for the treatment of different types of primary and metastatic cancers.

Methods and materials

Cell lines and culture

MDA-MB-231 human breast cancer cell line was obtained from Dr. Patricia Steeg at the National Cancer Institute (described in [22, 23]) and from American Type Culture Collection (Manassas, VA). Cells were cultured in Dulbecco's-modified Eagle's medium mixed 1:1 (v:v) with Ham's F-12 medium (DMEM/F12, Invitrogen, Carlsbad, CA) supplemented with 10% fetal bovine serum (FBS, Atlanta Biologicals, Lawrenceville, GA). Neither antibiotics nor anti-mycotics were used. All cell lines

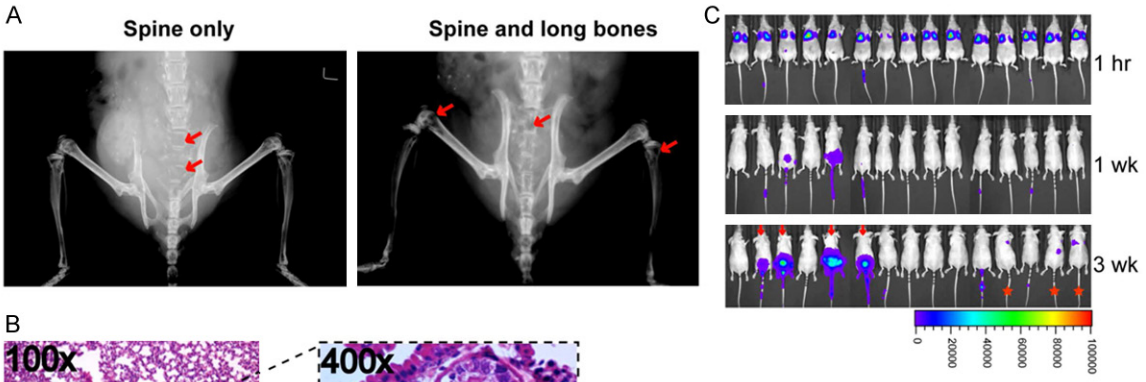

D

	Bone Metastasis (%)
1,000,000 cells	2/9 mice (22.2%)
500,000 cells	0/5 mice (0%)
250,000 cells	0/5 mice (0%)
100,000 cells	0/5 mice (0%)

E

	Bone Metastasis (%)	Lung Metastasis (%)	Disease-free (%)
MDA-MB-231 (ATCC)	0/10 mice (0%)	0/10 mice (0%)	10/10 mice (100%)
MDA-MB-231 (NCI)	1/10 mice (10%)	2/10 mice (20%)	7/10 mice (70%)
MDA-MB-231 (MCH)	1/10 mice (10%)	5/10 mice (50%)	4/10 mice (40%)
MDA-MB-231-LUC (MCH)	2/9 mice (22.2%)	2/9 mice (22.2%)	5/9 mice (55.6%)

Figure 1. MDA-231 cells form a low percentage of *bona fide* bone metastasis following intravenous route of cell delivery. A. X-Ray imaging revealed severe osteolysis of lumbar spine, femur, and tibia within 3-6 weeks post-inoculation of MDA-231 or MDA-231-LUC cells (arrows). B. Histological (Hematoxylin & Eosin) examination of lung and bone tissues collected at necropsy confirmed presence of metastatic foci at these sites. C. Longitudinal study of 15 animals injected with 1×10^6 MDA-231-LUC cells. Evidence of bone metastasis was detected as early as 1 week (arrows), while lung metastases were detected around week 3 (stars) post-injection. D. A limiting-dilution experiment of 10^5, 2.5×10^5, 5×10^5, or 10^6 cells injected iv. E. MDA-231 cells obtained from NCI, but not from ATCC, can form metastatic lesions through iv injection model.

were routinely tested and found to be negative of *Mycoplasma* spp. contamination. Cells were routinely passaged using 0.2 mmol/L EDTA in Ca^{2+}-free, Mg^{2+}-free, and $NaHCO_3$-free Hank's balanced salt solution (HBSS, Invitrogen). Cell lines were validated by STR DNA fingerprinting using the AmpFlSTR Identifiler kit according to manufacturer instructions (Applied Biosy-s tems). The STR profiles were compared to known ATCC fingerprints (ATCC.org), to the Cell Line Integrated Molecular Authentication database (CLIMA) version 0.1.200808 (Nucleic Acids Research 37: D925-D932 PMCID: PMC-2686526) and to the MD Anderson fingerprint database. The STR profiles matched known DNA fingerprints or were unique. Stable luciferase expression was achieved by lentiviral infection with particles carrying firefly luciferase/green fluorescent protein fusion gene, followed by two rounds of cell sorting by fluorescence activated cell sorter (FACS).

Western blot

Briefly, cells were lysed in RIPA buffer (25 mM Tris-HCL pH 7.6, 150 mM NaCl, 1% NP-40, 1% sodium deoxycholate, and 0.1% SDS, supplemented with protease and phosphatase inhibitors), and protein concentrations approximated with BCA assay (Pierce, Rockford, IL). Cell lysates were resolved on precast 4-15% SDS-PAGE (BioRad, Hercules, CA) under constant voltage conditions. Gels were blotted onto

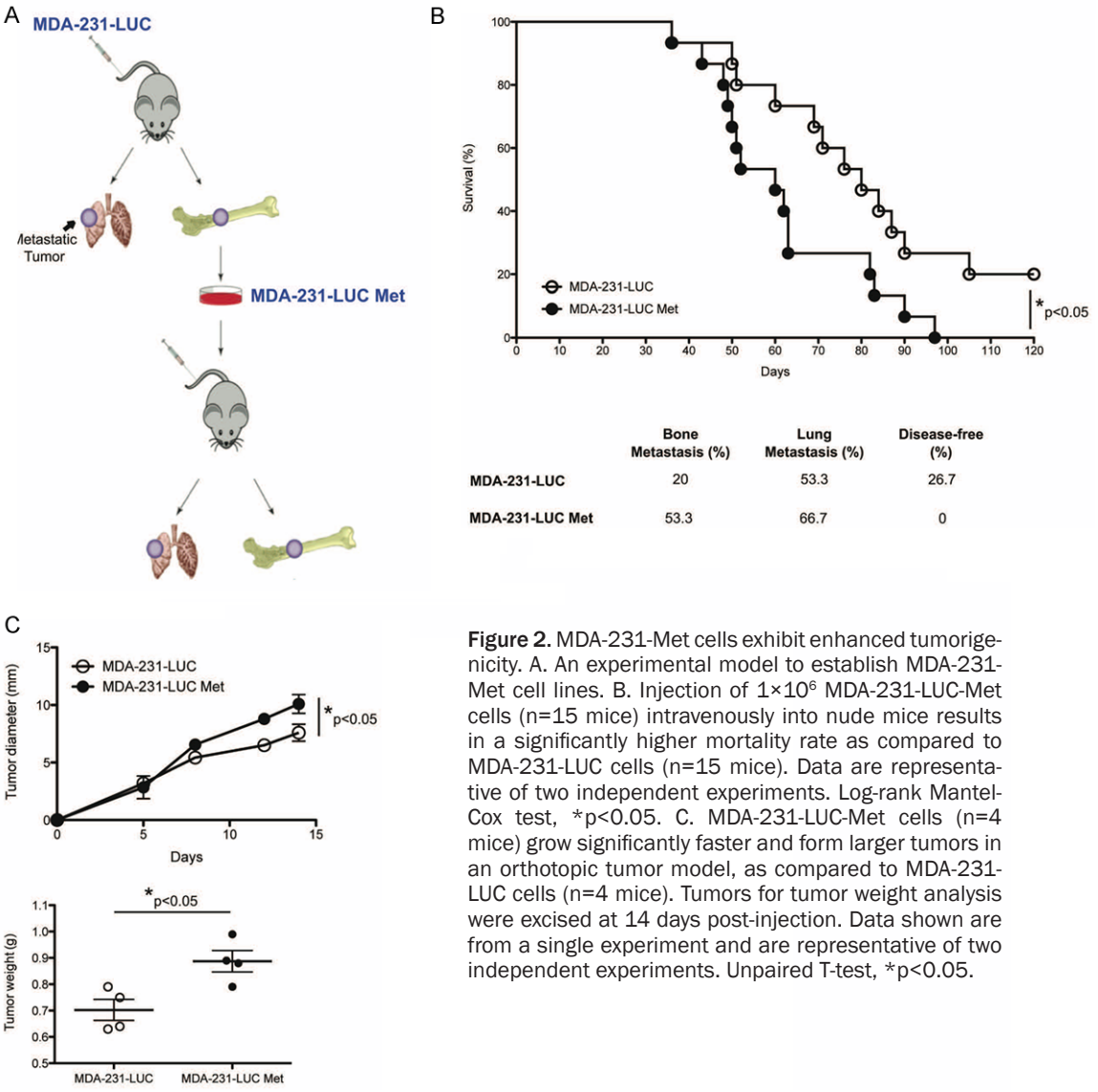

	Bone Metastasis (%)	Lung Metastasis (%)	Disease-free (%)
MDA-231-LUC	20	53.3	26.7
MDA-231-LUC Met	53.3	66.7	0

Figure 2. MDA-231-Met cells exhibit enhanced tumorigenicity. A. An experimental model to establish MDA-231-Met cell lines. B. Injection of 1×10^6 MDA-231-LUC-Met cells (n=15 mice) intravenously into nude mice results in a significantly higher mortality rate as compared to MDA-231-LUC cells (n=15 mice). Data are representative of two independent experiments. Log-rank Mantel-Cox test, *p<0.05. C. MDA-231-LUC-Met cells (n=4 mice) grow significantly faster and form larger tumors in an orthotopic tumor model, as compared to MDA-231-LUC cells (n=4 mice). Tumors for tumor weight analysis were excised at 14 days post-injection. Data shown are from a single experiment and are representative of two independent experiments. Unpaired T-test, *p<0.05.

PVDF membrane and blocked in 5% non-fat dry milk. Membranes were incubated in primary antibody overnight at 4°C. Following incubation with the secondary antibody, membranes were developed using chemiluminescent substrate kit (Pierce). Signal was detected by exposing membranes to X-Ray film. Band intensity was analyzed by densitometry using NIH ImageJ software, and all experiments were done in triplicate.

In vivo xenograft assays

Athymic nude mice 3-4 weeks old (Swiss nu-nu/Ncr) were purchased from the MD Anderson breeding core facility and housed under sterile conditions. All animal experiments were performed in accordance with IACUC regulations under MDACC-approved protocol. Briefly, cells were counted and re-suspended in HBSS for injection into mice. For mammary fat pad injections, 1×10^6 cells in final volume of 50 µl were injected. Tumors were measured (length×width) twice per week with manual calipers for 3 weeks. Mean tumor diameter was calculated using [square root of (length×width)] equation. For intravenous (tail vein) injections, 1×10^6 cells in final volume of 200 µl were injected, unless indicated otherwise. Mice injected with cells stably expressing luciferase were monitored by weekly bioluminescence imaging on Xenogen IVIS (Caliper, Waltham, MA), and bone lesions were confirmed by X-Ray.

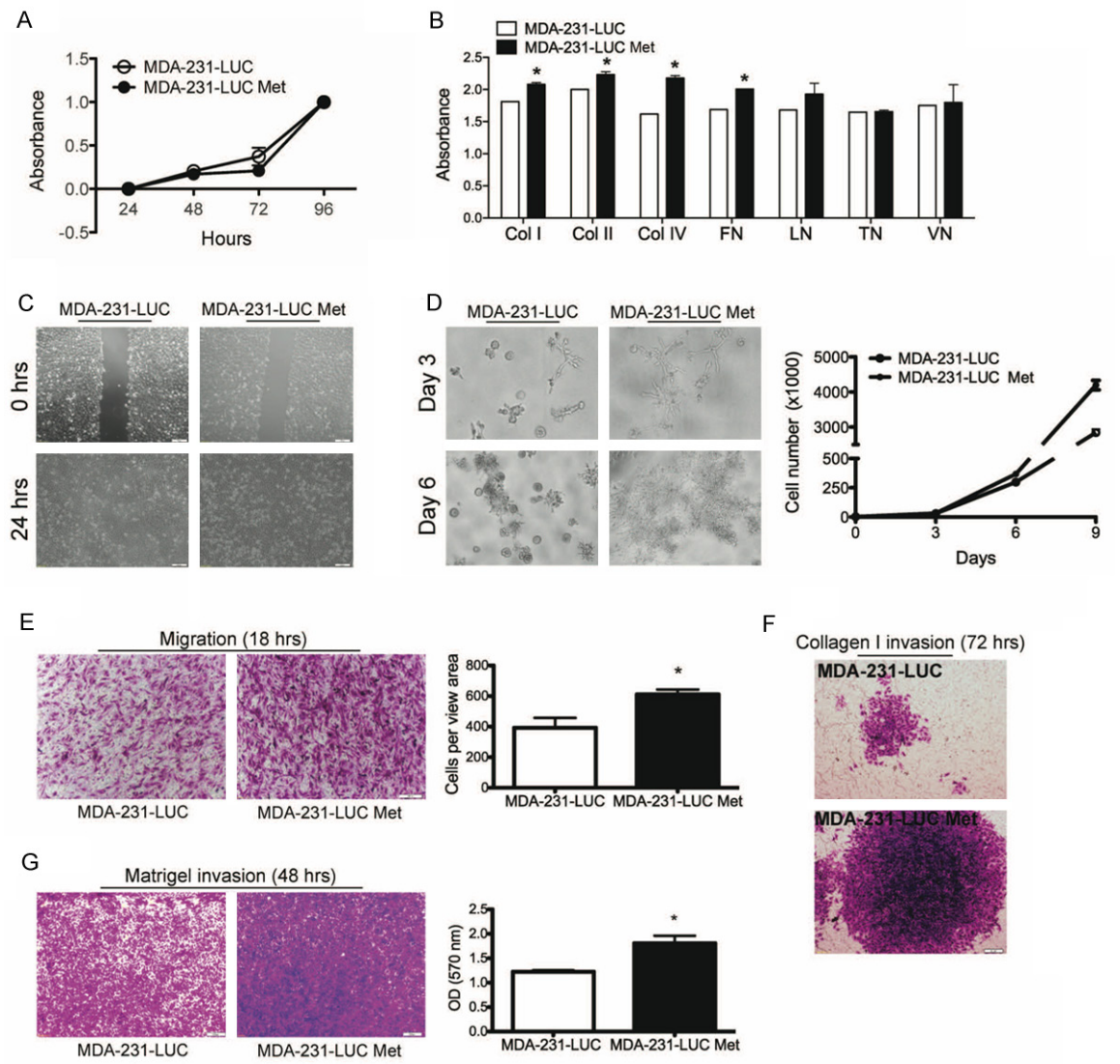

Figure 3. MDA-231-Met cells are highly invasive, but exhibit similar proliferation rate as compared to parental MDA-231 cells. A. MTT assay comparing proliferation of MDA-231-LUC and MDA-231-LUC-Met cells. Data are representative of two independent experiments performed in triplicate. B. Adhesion of MDA-231-LUC and MDA-231-LUC-Met cells to different types of extracellular matrix was measured. Data shown are mean ± SEM. T-test, *p<0.05. C. MDA-231-LUC and MDA-231-LUC-Met cells were grown to confluence. The monolayer was then scratched, and wound-healing ability assessed at 24 hours post-wounding. D. Same number of MDA-231-LUC and MDA-231-LUC-Met cells were plated under 3D conditions in Matrigel. To quantify proliferation, Matrigel was digested and cell number counted using hemacytometer. Data shown are mean ± SEM. Data are representative of three independent experiments performed in triplicate. T-test, *p<0.05. E. Migration of the same number of MDA-231-LUC and MDA-231-LUC-Met cells suspended in serum-free media was assayed at 18 hours post-plating. Migrated cells were photographed at low magnification and manually counted. Data shown are mean ± SEM. Data are representative of two independent experiments done in triplicate. T-test, *p<0.05. F. Invasion of MDA-231-LUC and MDA-231-LUC-Met cells through collagen I-coated membrane was assayed at 72 hours. Data are representative of triplicate experiments. G. Invasion of MDA-231-LUC and MDA-231-LUC-Met cells through Matrigel-coated membrane was assayed at 48 hours. Invaded cells were stained with crystal violet, photographed at a low magnification, lysed, and dye absorbance measured. Data shown are mean ± SEM. Data are representative of triplicate experiments. T-test, *p<0.05.

Immunohistochemistry

Matched pairs of human primary breast cancer and corresponding metastatic tumors were stained for phospho-S6 (Cell Signaling, Danvers, MA). Staining intensity and the number of cells exhibiting positive staining was analyzed by DAKO image analysis software

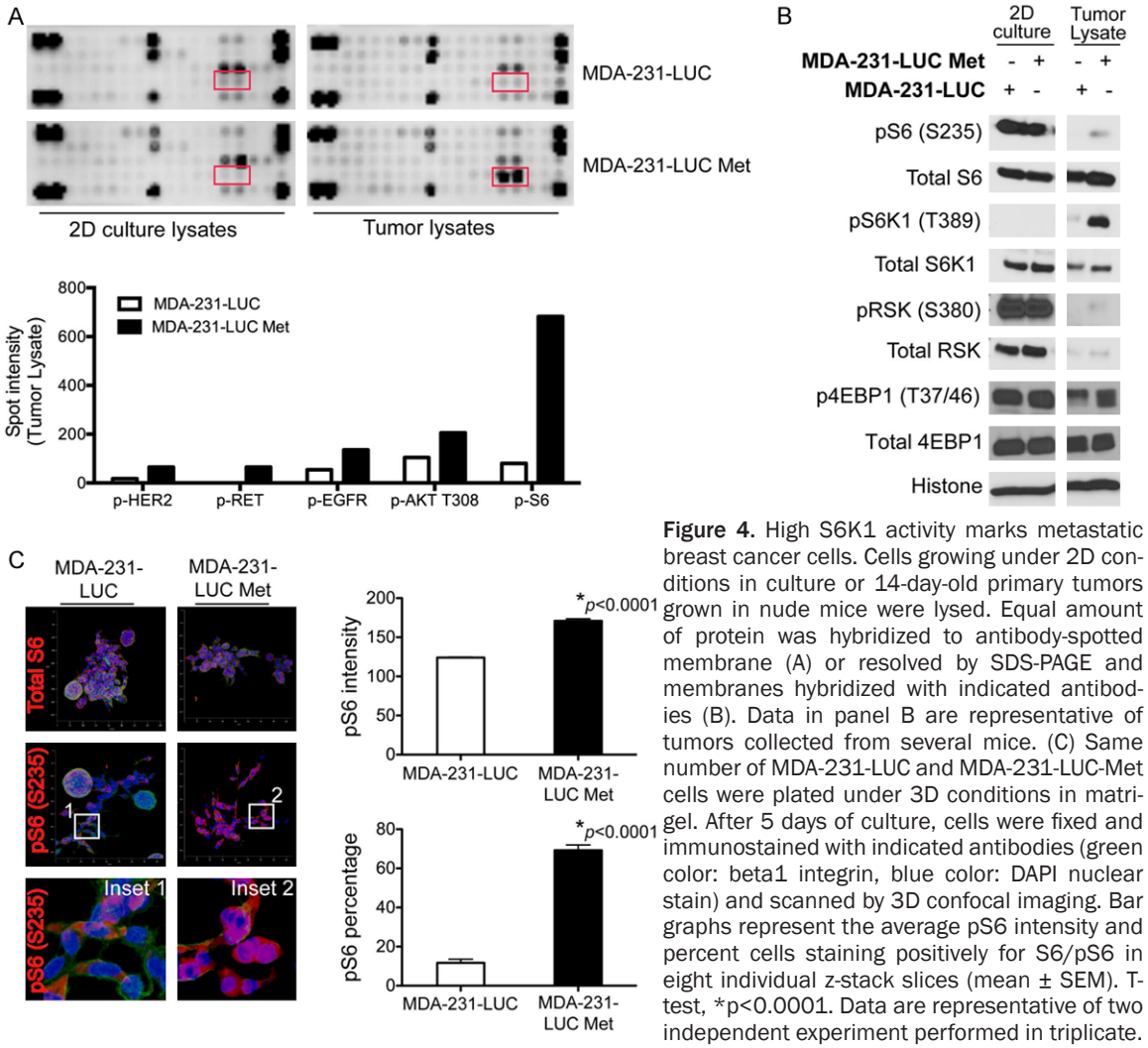

Figure 4. High S6K1 activity marks metastatic breast cancer cells. Cells growing under 2D conditions in culture or 14-day-old primary tumors grown in nude mice were lysed. Equal amount of protein was hybridized to antibody-spotted membrane (A) or resolved by SDS-PAGE and membranes hybridized with indicated antibodies (B). Data in panel B are representative of tumors collected from several mice. (C) Same number of MDA-231-LUC and MDA-231-LUC-Met cells were plated under 3D conditions in matrigel. After 5 days of culture, cells were fixed and immunostained with indicated antibodies (green color: beta1 integrin, blue color: DAPI nuclear stain) and scanned by 3D confocal imaging. Bar graphs represent the average pS6 intensity and percent cells staining positively for S6/pS6 in eight individual z-stack slices (mean ± SEM). T-test, *p<0.0001. Data are representative of two independent experiment performed in triplicate.

(Carpinteria, CA) in 10 randomly chosen fields for each slide. Images were taken using CarlZeiss inverted Stemi 2000-C microscope (Axiovision software package). Data shown are mean ± SEM. All experiments were performed under the Institutional Review Board-approved protocol.

MTT assay

Cells were seeded in quadruplicate for each condition, in a 96-well plate. At set time points, MTT (3-[4,5-dimethylthiazol-2-yl]-2,5 diphenyl tetrazolium bromide) solution (Sigma-Aldrich, St. Louis, MO) was added to wells and incubated at 37°C for 4 hours. MTT solution was then removed and DMSO was added to solubilize formazan dye. Absorbance at 540 nm was measured using a Synergy H4 microplate reader (BioTek, Winooski, VT).

Adhesion assay

Cell adhesion kit was purchased from Millipore (Billerica, MA). The assay was carried out as per the manufacturer's recommendations and as previously described [30].

Wound healing assay

Same number of cells were plated in triplicate onto 6-well plates and allowed to grow to confluence. Cell monolayer was scratched with a pipette tip to create a "wound", and wound closure was examined after 24 hours.

3D Matrigel mammosphere assay

Growth factor-reduced Matrigel was purchased from BD Biosciences (San Jose, CA). The assay worked reproducibly when Matrigel protein concentration was over 9 mg/ml. Experiments

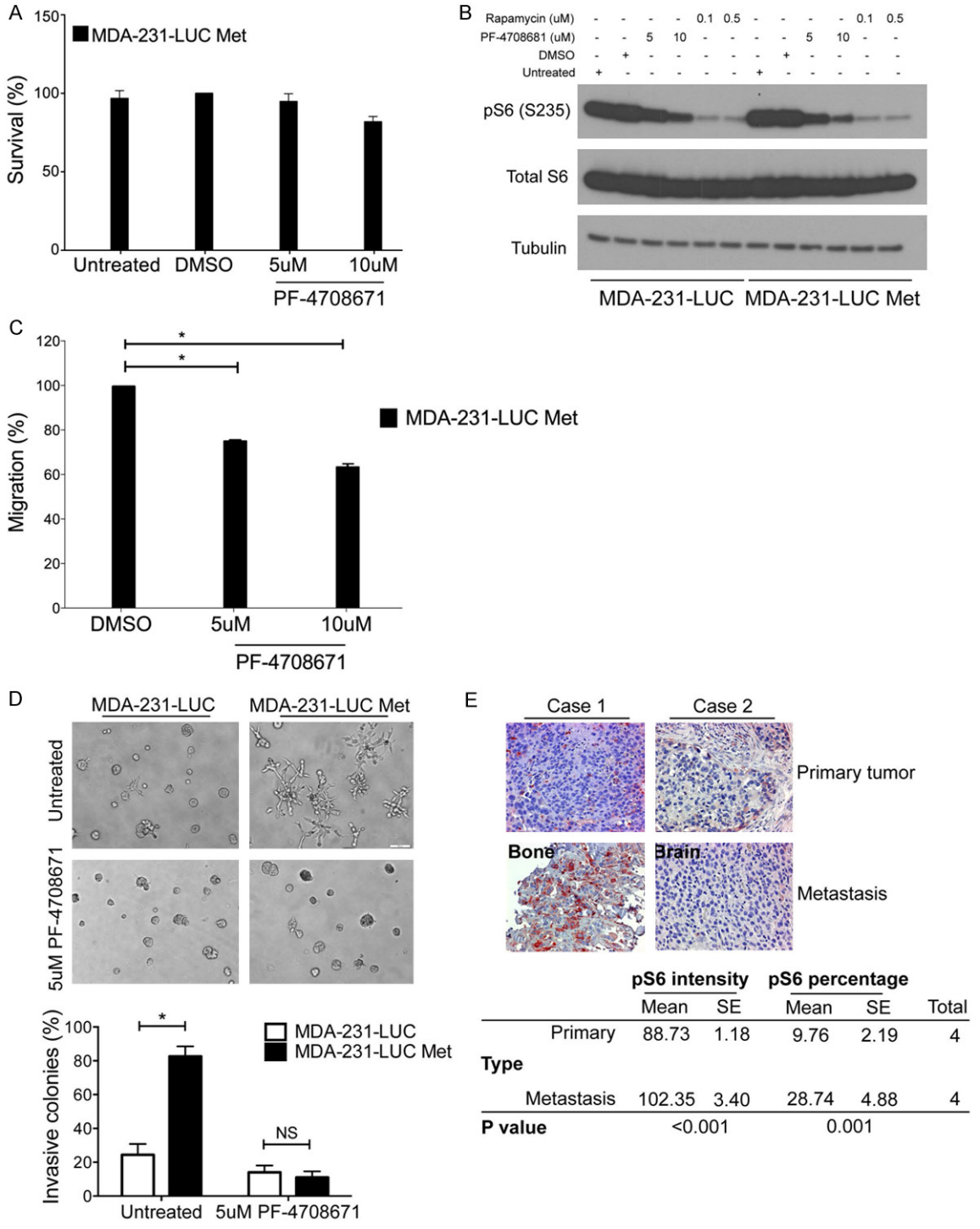

	pS6 intensity		pS6 percentage		
	Mean	SE	Mean	SE	Total
Primary	88.73	1.18	9.76	2.19	4
Type					
Metastasis	102.35	3.40	28.74	4.88	4
P value	<0.001		0.001		

Figure 5. Targeting S6K1 with PF-4708671 inhibitor strongly inhibits cell migration and invasion without affecting their proliferation. A. MDA-231-LUC-Met cells were treated with 5 uM or 10 uM PF-4708671. Cell proliferation was measured after 24 hours. Data shown are mean ± SEM. B. Cells were treated for 24 hours with indicated concentrations of the drugs. Rapamycin treatment served as positive control for inhibition of S6 phosphorylation. Lysed samples were resolved by SDS-PAGE and membranes hybridized with indicated antibodies. C. Migration of MDA-231-LUC-Met cells suspended in serum-free media with or without S6K1 inhibitor treatment was assayed at 24 hours post-plating. Crystal violet was extracted from migrated cells and absorbance was measured. Data shown are mean ± SEM. Data are representative of two independent experiments performed in triplicate. T-test, *p<0.05. D. Cells were plated in 3D Matrigel as before and treated once on day 0 with 5 uM PF-4708671. Data shown are mean ± SEM. Data are representative of three independent experiments done in triplicate. E. Matched primary

and metastatic breast cancer tumor samples collected from the same patient (n=4 patients) were analyzed by immunohistochemistry for expression of S6 protein phosphorylated on Ser235. Data were quantified by analyzing 10 independent fields per section and shown as mean ± SEM. T-test, *p<0.001.

were carried out as previously described [31, 32], and were performed in triplicate. For immunocytochemistry, cells growing in 3D cultures were fixed with 4% paraformaldehyde and stained for S6 and phospho-S6 (Cell Signaling, Danvers, MA). Cells were examined on CarlZeiss LSM 710 confocal microscope with ZEN 2009 software.

Migration assay

Transwell inserts (8 um pore size) were purchased from BD Biosciences (San Jose, CA). Tumor cells were suspended in serum-free culture media, and culture media supplemented with 10% FBS was used as a chemoattractant. All experiments were performed in triplicate.

Collagen I invasion assay

Collagen I invasion assay kit was purchased from Millipore (Billerica, MA) and assays carried out as per the manufacturer's protocol.

Matrigel invasion assay

Transwell inserts pre-coated with Matrigel were purchased from BD Biosciences (San Jose, CA). Tumor cells were suspended in serum-free culture media, and culture media supplemented with 10% FBS was used as a chemoattractant. Assays were carried out as per the manufacturer's instructions and performed in triplicate.

Kinase array

PathScan Receptor Tyrosine Kinase signaling antibody array kit (cat. #7982) was purchased from Cell Signaling (Danvers, MA) and was utilized as per manufacturer's instructions. To prepare tumor lysates, snap-frozen tumor tissues were lysed in the lysis buffer provided with the kit, followed by sonication. Protein concentration was assayed, and equal amount of total protein was loaded for each sample. To determine spot intensity, doublet spots for each target protein were scanned by ImageJ software.

Statistical analysis

Statistical analyses were performed using Student's T-test unless indicated otherwise and $p<0.05$ was deemed significant.

Results

Intravenous injection of MDA-MB-231 cells results in a low percentage of bone metastasis in addition to lung metastasis

We recently observed that following an intravenous injection of 1×10^6 MDA-231 cells into athymic nude mice, a low percentage of animals developed rapid and very aggressive bone metastasis. This finding was entirely unexpected, as MDA-231 has been used in experimental metastasis assays for decades, and yet the only reported outcome of such studies was lung metastasis [21, 33, 34]. Although we suspected that these large tumors were bone metastases because many animals consequently developed hind leg paralysis, we confirmed that these animals exhibited osteolysis typically associated with breast cancer bone metastasis. As X-Ray images revealed, most animals affected by bone metastasis in this model show evidence of severe osteolysis of the lumbar spine, though some also developed osteolytic fractures of femur or tibia (**Figure 1A**, arrows). The presence of metastatic lesions in lungs and bones of these mice was further confirmed by immunohistochemical (IHC) staining (**Figure 1B**).

As shown by bioluminescence imaging in **Figure 1C**, immediately following the intravenous tail vein injection of luciferase-tagged MDA-231 cells, bioluminescent signal was restricted to the lungs (**Figure 1C**, upper panel). One week later, bioluminescence was detected in the spine and hind legs of some animals (**Figure 1C**, middle panel), whereas lung bioluminescence did not begin to reappear until week 3 (**Figure 1C**, lower panel). These data suggest that MDA-231 cells are heterogeneous and may contain a clonogenic cell population capable of establishing rapid bone metastasis associated with aggressive TNBC disease progression.

To determine frequency of cells within the parental MDA-231 cell population that were capable of forming bone metastases, we performed a limiting dilution-type animal experiment, where different numbers of cells were

injected intravenously in the same total volume of diluent. The results indicate that the frequency of cells capable of forming rapid bone metastasis was about 1 in 0.5-1×10^6 cells (**Figure 1D**). Finally, there are many MDA-231 cell line variants, but not every variant we tested had the same characteristics of *in vivo* behavior. As shown in **Figure 1E**, with the exception of MDA-231 cells from ATCC, all other MDA-231 variants tested exhibited similar metastatic behavior. Furthermore, all cells were subjected to "finger printing" analysis based on a 9-allele pattern (see Materials and Methods) and all were identified as "MDA-MB-231" cells, matching ATCC profile. These data confirm what many others had already described: the MDA-231 cell line is highly heterogeneous [17, 19, 35, 36]. Our results also suggest that there may exist a subpopulation of highly aggressive cells capable of forming rapid bone metastasis.

Isolation and characterization of MDA-231-LUC-Met cells that exhibit enhanced tumorigenic and metastatic potential

Based on our hypothesis that the rapid bone metastasis we observed were formed by a clonogenic subpopulation of cells present in the parental MDA-231 cell line, we then proceeded with isolation and characterization of this subpopulation. We followed the experimental procedure outlined in **Figure 2A**: MDA-231 cells stably expressing luciferase (MDA-231-LUC) were injected intravenously through the tail vein and animals were monitored for development of bone metastasis. We then used a needle biopsy procedure to aspirate cells from a metastatic bone tumor and expanded them in culture. We chose not to follow the same procedure for isolation of cells from lung metastasis because these studies had been done previously by others [35]. Upon cell expansion *in vitro*, newly isolated MDA-231-LUC-Met cells were subjected to cytologic "fingerprinting" and karyotyping to ensure absence of contaminating mouse cells. We found MDA-231-LUC-Met cells to be negative of mouse stroma contamination and to exhibit gene clustering that matched the MDA-MB-231 profile from ATCC (data not shown).

Upon *in vivo* cell line comparison, we found the newly isolated MDA-231-LUC-Met cells to be more tumorigenic and metastatic than their parental MDA-231-LUC counterparts. Animals injected with MDA-231-LUC-Met cells died more rapidly than those injected with MDA-231-LUC cells (median survival 60 vs. 80 days, respectively, **Figure 2B**). Moreover, over a 120-day experiment, animals injected with MDA-231-LUC-Met cells exhibited a higher incidence of bone metastasis, as well as lung metastasis (**Figure 2B**). Hence, we conclude that MDA-231-LUC-Met cells retain their heterogeneity and maintain ability to colonize both bone and lung in this experimental metastasis model.

To further characterize these cells, we performed an orthotopic mammary fat pad injection experiment. Interestingly, we found that while injection of MDA-231-LUC-Met cells resulted in accelerated tumor growth and larger tumor size when compared to MDA-231-LUC cells (**Figure 2C**), *in vitro* proliferation of these cell lines was indistinguishable (**Figure 3A**). Additionally, there were only minor (12-20%) differences in adhesion of these cells to various types of extracellular matrix (**Figure 3B**), and no appreciative differences in colony formation, anchorage-independent growth, and wound-healing assays (data not shown and **Figure 3C**).

A recent shift in opinion of usefulness of *in vitro* assays points in the direction of three-dimensional (3D) assays as being more representative of *in vivo* cell behavior, as compared to cells grown on plastic in 2D. Hence, when we tested behavior of MDA-231-LUC and MDA-231-LUC-Met cells in 3D Matrigel culture, we observed two distinct phenotypes that correlate with our *in vivo* findings: in 3D, MDA-231-LUC-Met cells were highly invasive and proliferated at a higher rate, when compared to MDA-231-LUC cells (**Figure 3D**). Their enhanced invasive ability was further confirmed in Boyden chamber-type assays, with similar results obtained with uncoated membranes or membranes coated with Collagen I or Matrigel (**Figure 3E-G**). Together, these data indicate that MDA-231-LUC-Met cells are highly invasive and proliferate at a higher rate when grown in the presence of extracellular matrix, all of which may attribute to their enhanced metastatic potential.

Kinase array reveals hyper-activation of the Akt/mTOR/S6K1 axis in MDA-231-LUC-Met cells

In order to elucidate a potential molecular mechanism responsible for accelerated MDA-

231-LUC-Met metastasis and to determine "druggable" protein targets, we subjected cell lysates collected from cells grown in 2D *in vitro* culture and lysates of primary orthotopic tumors to a phospho-kinase antibody array. We chose to utilize this type of array because majority of anti-cancer drugs already in the clinic or undergoing pre-clinical testing are kinase inhibitors. As expected, MDA-231-LUC and MDA-231-LUC-Met cells grown under 2D conditions exhibited few differences in activation of kinase pathways (**Figure 4A**, left panel). This supports our earlier conclusion that MDA-231-LUC-Met cells exhibit behavioral differences only in the presence of extracellular matrix or within a tumor microenvironment that provides additional growth factors or cytokines that activate specific signaling pathways within these cells (**Figure 3D-G**). We then tested lysates prepared from freshly collected primary tumors formed by these two cell lines (**Figure 4A**, right panel). Surprisingly, we only observed one major difference in activation of kinase pathways between these two cell lines: a 9-fold elevation in phosphorylation of Ser235/236 of RPS6 (**Figure 4A**). This led us to ask if either of the two upstream kinases, p90RSK or p70S6K that can phosphorylate RPS6 at Ser235/236, are hyper-activated in these tumor cells. Interestingly, only phosphorylation at Thr389 of S6K1 was elevated in these tumors (**Figure 4B**). Moreover, we observed that Akt signaling upstream of mTORC1 and S6K1, but not ERK1/2 signaling upstream of RSK, was elevated in these tumor lysates (**Figure 4A**, bar graph). Phosphorylation of another target of mTORC1, 4EBP1, was also elevated in tumors formed by the MDA-231-LUC-Met cells (**Figure 4B**). Together, these results indicated hyper-activation of the Akt/mTORC1/S6K1 pathway leading to a marked enhancement in phosphorylation of the ribosomal protein S6 at Ser235/236.

To validate the kinase array data we obtained from tumor lysates, we asked whether phosphorylation of ribosomal protein S6 was also elevated in MDA-231-LUC-Met cells grown *in vitro* under 3D Matrigel conditions. As shown in **Figure 4C**, confocal imaging revealed enhanced S6 phosphorylation in MDA-231-LUC-Met cells grown under 3D conditions. Confocal analysis also indicated that majority of MDA-231-LUC-Met cells stained positive for phospho-S6, while its expression in parental MDA-231-LUC cells was heterogeneous and few cells exhibited strong staining intensity. This indicates that the MDA-231-LUC-Met variant line is enriched in cells that display hyper-activation of the mTOR/S6K1 pathway upstream of RPS6.

Various studies have described the role of mTOR in cell motility, specifically through activation of S6K1 and 4EBP1 [37]. To determine the functional importance of S6K1 in the metastatic properties of MDA-231-LUC-Met cells, we treated parental or metastatic cells with PF-4708671, a selective small molecule inhibitor of S6K1. As shown in **Figure 5A**, treatment of MDA-231-LUC-Met cells with 5 or 10 μM concentration of PF-4708671 for 24 hours was not cytotoxic. At the same time, treatment of cells with 5 and 10 μM PF-4708671 resulted in decreased phosphorylation of S6 (**Figure 5B**). In a Boyden chamber migration assay, treatment of MDA-231-LUC-Met cells with PF-4708671 for 24 hours inhibited cell migration by up to 40% (**Figure 5C**). Interestingly, treatment of cells grown in 3D Matrigel culture with PF-4708671 yielded even more dramatic results: migration of MDA-231-LUC-Met cells was inhibited by 86.7% (**Figure 5D**). Together, these data indicated that targeting S6K1 activity might be beneficial in an adjuvant setting to prevent metastasis. To this end, we then validated clinical importance of S6K1 activation in the context of breast cancer metastasis. We stained 8 paired (primary and metastatic tissues collected from the same patient) breast cancer samples collected from primary and metastatic tumors for RPS6 Ser235/236 phosphorylation. As shown in **Figure 5E**, both the intensity and percentage of phospho-S6 positive cells were significantly increased in 3/4 cases of human metastatic breast cancer, as compared to their matched primary tumors. As is the case with parental (MDA-231-LUC) and metastatic (MDA-231-LUC-Met) cell lines grown under 3D conditions (**Figure 4C**), there was a 3-fold difference in the percentage of phospho-S6 positive cells present in metastatic tumors (**Figure 5E**). We believe these data indicate that there may be a clonogenic population of highly metastatic, S6K1-activated cells responsible for early TNBC relapse.

Discussion

Cancer metastases remain an important health issue to most individuals affected by the dis-

ease. In breast cancer, patients diagnosed with an early-stage, non-invasive disease have an excellent 5-year survival rate of over 98%, which plummets to under 25% upon diagnosis of distant metastases [http://seer.cancer.gov/csr/1975_2010/]. Moreover, current therapeutic approaches in the metastatic breast cancer setting are palliative and no curative strategies have been approved at this time. Consequently, patients with distant metastases are subject to long-term, chronic disease management. Multiple hypotheses exist as to why metastases treatment is lagging, including existence of relatively few effective animal models of metastasis to study the disease progression in a research setting [12], molecular changes that occur within the metastatic tumor landscape [38], and ineffective clinical trial design that negatively selects against potential anti-metastatic therapeutic agents [39, 40].

Our current report describes a new mouse model of breast cancer metastasis, which allows study of concurrent skeletal metastases and metastasis to lungs, liver, and other soft tissues in immunocompromised athymic mice. The major advantages of this model as compared to other models of breast cancer metastasis to bone are ease of execution of tail vein injections, utilization of relatively inexpensive athymic nude mice, and rapid disease onset. Specifically, while injection of breast cancer cells into the left ventricle of the heart is a highly reproducible, well-established model of bone metastasis, it is also technically challenging and may result in high animal mortality associated with the procedure itself [41]. At the same time, intracardiac injection of cells produces metastasis mostly to bone and brain within 4-6 weeks, but infrequently to the lungs and other soft tissues [12, 13]. Moreover, use of the intracardiac injection model requires deep anesthesia, which could further decrease animal survival. Conversely, our model is easily executed; cells could be injected rapidly without use of the anesthesia, and with low potential mortality rate. In addition, in this study we show that the intravenous injection of MDA-231-LUC-Met cells produces rapid metastases to bone and soft tissues within the same cohort of animals, which should provide a valuable resource for expedited testing of potential anti-metastatic therapeutics.

The second advantage of this model is use of well-characterized athymic nude mice as recipients of the highly metastatic MDA-231-LUC-Met cells. Recent advances in derivation and characterization of new genetic backgrounds of immunocompromised mice have allowed for establishment of hybrid “humanized” mouse models to study the behavior of human cancer cells in the human bone microenvironment [15, 42, 43], while other models looked for spontaneous metastases to bone from orthotopically injected tumor cells [44]. Yet, the major disadvantage of these models lies in the astronomical cost of the highly immunosuppressed mice used in these studies, such as the non-obese diabetic severe combined immunodeficient (NOD/SCID) and NOD/SCID gamma (NSG) mice, which typically cost around three times as much as the athymic nude mice. Together, we believe use of the less expensive animals will provide private investigators more freedom in testing their hypotheses aimed at reducing metastatic breast cancer morbidity and mortality.

Finally, our model provides great scientific flexibility to modulate gene expression in low metastatic MDA-231-LUC and highly metastatic MDA-231-LUC-Met clones. As we have characterized both the time to metastases onset and the pattern of anatomical metastasis distribution, this model will provide a useful tool for investigators interested in comparing a particular gene’s role on metastases onset and/or their specific anatomical “homing” capacity.

Although we only utilize a single cell line, the MDA-MB-231, which has already been extensively studied by many others in the context of bone metastasis [12, 18, 19], our model still holds potential to elucidate additional molecular mechanisms that underlie metastasis. For instance, even though bone-homing MDA-231 cells have been characterized and a bone metastasis signature established [18, 19], there are several clinical reports that identify discordance between the gene signature identified through the animal models and the gene signature that exists in breast cancer patients [45-47]. Moreover, therapeutic interventions derived from such studies have not shown significant benefit for patients suffering from breast cancer metastases [48, 49]. These data suggest that perhaps not all potential predictors of bone metastases had been identified to date. We hope that this model will be useful in providing better characterization of primary

tumors and their propensity for forming metastasis.

In terms of identification of potentially "targetable" proteins by our model, we identified that the kinase S6K1 is highly important in these metastatic breast cancer cells. We further showed that pharmacological inhibition of S6K1 function exerts an inhibitory effect on tumor cell migration. Although S6K1 is directly downstream of a well-known mTORC1 complex with strong ties to metastasis regulation, to date, few reports have attempted to delineate specific S6K1 functions related to metastasis. S6K1 has previously been implicated in breast cancer progression: its mRNA and protein levels are highly elevated in primary breast cancers and correlate with poor patient survival [29, 50, 51]. Moreover, a recent study showed that inhibition of S6K1 kinase activity in TNBC leads to decreased local tumor relapse, whereas modulation of mTORC1 function with clinically-approved rapalogs did not yield similar results [52]. In accordance with our results that S6K1 function was highly elevated in the invasive breast cancer cells, Segatto et al. concluded that S6K1 function was required for cell survival within the tumor microenvironment and subsequent tumor re-growth [52]. In addition, S6K1 copy number gain significantly correlates with increased risk of distant recurrence in breast cancer patients [53].

In vitro studies have showed that S6K1 is a mediator of cell motility in response to a variety of growth factors such as EGF, HGF and IGF-1 [54-56]. In addition to changes in Akt and S6 phosphorylation, the kinase array that we performed on tumor samples from MDA-231-LUC-Met cells also showed an increase in phosphorylation of EGFR, HER2 and RET. There is an indication that EGFR function and breast cancer metastasis to bone and brain are linked, and it is now known that high expression of RET inversely correlates with metastasis-free survival in breast cancer [57-59]. Since the ErbB and RET receptors are upstream of PI3K-Akt, it is plausible that hyper-activation of the Akt/mTOR/S6K1 axis is prompted by activation of these receptors by their ligands in the tumor microenvironment [60, 61]. So far, EGFR inhibition has showed only limited promise in the treatment of metastatic TNBC, possibly due to alterations in components of signaling pathways downstream of EGFR, such as KRAS mutation or loss of PTEN [62]. The only way to overcome this problem is to identify 'druggable' targets that are further downstream in these pathways.

In conclusion, our model described in this report and previous models of breast cancer bone metastasis all converge upon the mTORC1 pathway as the major signaling transduction node responsible for controlling metastasis [29, 63]. Consequently, clinical benefits of inhibitors to mTORC1 and PI3 kinases, all acting directly upstream of the S6K, were highly anticipated in metastatic breast cancer. Yet, to date, those inhibitors have proved ineffective [64-66]. Pharmaceutical companies have recently showed interest in the development of S6K inhibitors and dual S6K/Akt inhibitors, with several of these products currently in the pipeline [24]. An ATP-competitive S6K inhibitor from Eli Lilly, LY2584702 tosylate, did not perform satisfactorily in a Phase Ib clinical trial [67]. XL418 from Exelixis was the first dual S6K/Akt inhibitor to enter clinical trial for solid cancers in 2007. However, the trial was suspended due to low drug exposure [24]. Another dual S6K/Akt inhibitor MSC2363318A developed by EMD Serono is currently entering Phase 1 clinical trial for advanced malignancies [http://clinicaltrials.gov/]. Based on our data and the data described in [52], we propose that patients who exhibit the activation of S6K1 or high S6 phosphorylation in their primary tumors might be at a greater risk for developing local relapse and/or distant metastases. Hence, early treatment of these patients with S6K inhibitors in combination with the standard of care might provide a significant clinical benefit and prolong their disease-free survival.

Acknowledgements

The authors would like to thank Dr. Patricia S. Steeg (Women's Cancer Section, National Cancer Institute, Bethesda, MD) for providing the original MDA-MB-231 cell line. This study was funded in whole or in part by the following: National Institutes of Health (CA109311, CA099031, and CCSG CA16672); The University of Texas MD Anderson-China Medical University and Hospital Sister Institution Fund; Ministry of Health and Welfare, China Medical University Hospital Cancer Research Center of Excellence (MOHW103-TD-B-111-03; Taiwan), the Program

for Stem Cell and Regenerative Medicine Frontier Research (NSC 102-2321-B-039-001; Taiwan), International Research-Intensive Centers of Excellence in Taiwan (NSC 103-2911-I-002-303); Center for Biological Pathways; National Breast Cancer Foundation, Inc.; Patel Memorial Breast Cancer Research Fund; Department of Defense (DOD) Congressionally Directed Medical Research Breast Cancer Research Program (Postdoctoral Fellowship Award W81XWH-10-1-0749; to Y.B.K.); Andrew Sowell-Wade Huggins Graduate Fellowship (to A.G.); SEOM Translational Research Fellowship (to M.P.S). In memoriam, Mr. Tiong Loi Ang for his courageous fight against cancer.

Disclosure of conflict of interest

The authors declare no conflict of interest.

Address correspondence to: Mien-Chie Hung, Department of Molecular and Cellular Oncology, The University of Texas MD Anderson Cancer Center, Box 108, 1515 Holcombe Boulevard, Houston, TX 77030. Tel: 713-792-3668; Fax: 713-794-3270; E-mail: mhung@mdanderson.org

References

[1] Lin Y, Yin W, Yan T, Zhou L, Di G, Wu J, Shen Z, Shao Z and Lu J. Site-specific relapse pattern of the triple negative tumors in Chinese breast cancer patients. BMC Cancer 2009; 9: 342.

[2] Dent R, Trudeau M, Pritchard KI, Hanna WM, Kahn HK, Sawka CA, Lickley LA, Rawlinson E, Sun P and Narod SA. Triple-negative breast cancer: clinical features and patterns of recurrence. Clin Cancer Res 2007; 13: 4429-4434.

[3] Tseng LM, Hsu NC, Chen SC, Lu YS, Lin CH, Chang DY, Li H, Lin YC, Chang HK, Chao TC, Ouyang F and Hou MF. Distant metastasis in triple-negative breast cancer. Neoplasma 2013; 60: 290-294.

[4] Liedtke C, Mazouni C, Hess KR, Andre F, Tordai A, Mejia JA, Symmans WF, Gonzalez-Angulo AM, Hennessy B, Green M, Cristofanilli M, Hortobagyi GN and Pusztai L. Response to neoadjuvant therapy and long-term survival in patients with triple-negative breast cancer. J Clin Oncol 2008; 26: 1275-1281.

[5] Ihemelandu CU, Naab TJ, Mezghebe HM, Makambi KH, Siram SM, Leffall LD Jr, Dewitty RL Jr and Frederick WA. Basal cell-like (triple-negative) breast cancer, a predictor of distant metastasis in African American women. Am J Surg 2008; 195: 153-158.

[6] Jensen AO, Jacobsen JB, Norgaard M, Yong M, Fryzek JP and Sorensen HT. Incidence of bone metastases and skeletal-related events in breast cancer patients: A population-based cohort study in Denmark. BMC Cancer 2011; 11: 29.

[7] Yong M, Jenson AO, Jacobsen JB, Norgaard M, Fryzek JP and Sorensen HT. The Incidence of Bone Metastases and Skeletal-Related Events in Breast Cancer Patients: A Population-Based Cohort Study in Denmark (1999-2007). Cancer Res 2009; 69: 608S-609S.

[8] Berman AT, Thukral AD, Hwang WT, Solin LJ and Vapiwala N. Incidence and patterns of distant metastases for patients with early-stage breast cancer after breast conservation treatment. Clin Breast Cancer 2013; 13: 88-94.

[9] Irvin W Jr, Muss HB and Mayer DK. Symptom management in metastatic breast cancer. Oncologist 2011; 16: 1203-1214.

[10] Rosa Mendoza ES, Moreno E and Caguioa PB. Predictors of early distant metastasis in women with breast cancer. J Cancer Res Clin Oncol 2013; 139: 645-652.

[11] Koo JS, Jung W and Jeong J. Metastatic breast cancer shows different immunohistochemical phenotype according to metastatic site. Tumori 2010; 96: 424-432.

[12] Goldstein RH, Weinberg RA and Rosenblatt M. Of mice and (wo)men: mouse models of breast cancer metastasis to bone. J Bone Miner Res 2010; 25: 431-436.

[13] Yoneda T, Michigami T, Yi B, Williams PJ, Niewolna M and Hiraga T. Actions of bisphosphonate on bone metastasis in animal models of breast carcinoma. Cancer 2000; 88: 2979-2988.

[14] Nola S, Sin S, Bonin F, Lidereau R and Driouch K. A methodological approach to unravel organ-specific breast cancer metastasis. J Mammary Gland Biol Neoplasia 2012; 17: 135-145.

[15] Kretschmann KL and Welm AL. Mouse models of breast cancer metastasis to bone. Cancer Metastasis Rev 2012; 31: 579-583.

[16] Welch DR, Harms JF, Mastro AM, Gay CV and Donahue HJ. Breast cancer metastasis to bone: evolving models and research challenges. J Musculoskelet Neuronal Interact 2003; 3: 30-38.

[17] Kang Y, He W, Tulley S, Gupta GP, Serganova I, Chen CR, Manova-Todorova K, Blasberg R, Gerald WL and Massague J. Breast cancer bone metastasis mediated by the Smad tumor suppressor pathway. Proc Natl Acad Sci U S A 2005; 102: 13909-13914.

[18] Kang Y, Siegel PM, Shu W, Drobnjak M, Kakonen SM, Cordon-Cardo C, Guise TA and Massague J. A multigenic program mediating breast cancer metastasis to bone. Cancer Cell 2003; 3: 537-549.

[19] Minn AJ, Kang Y, Serganova I, Gupta GP, Giri DD, Doubrovin M, Ponomarev V, Gerald WL, Blasberg R and Massague J. Distinct organ-specific metastatic potential of individual breast cancer cells and primary tumors. J Clin Invest 2005; 115: 44-55.

[20] Price JE. Metastasis from human breast cancer cell lines. Breast Cancer Res Treat 1996; 39: 93-102.

[21] Yoneda T, Williams PJ, Hiraga T, Niewolna M and Nishimura R. A bone-seeking clone exhibits different biological properties from the MDA-MB-231 parental human breast cancer cells and a brain-seeking clone in vivo and in vitro. J Bone Miner Res 2001; 16: 1486-1495.

[22] Palmieri D, Bronder JL, Herring JM, Yoneda T, Weil RJ, Stark AM, Kurek R, Vega-Valle E, Feigenbaum L, Halverson D, Vortmeyer AO, Steinberg SM, Aldape K and Steeg PS. Her-2 overexpression increases the metastatic outgrowth of breast cancer cells in the brain. Cancer Res 2007; 67: 4190-4198.

[23] Yoneda T, Williams PJ, Hiraga T, Niewolna M and Nishimura R. A bone-seeking clone exhibits different biological properties from the MDA-MB-231 parental human breast cancer cells and a brain-seeking clone in vivo and in vitro. J Bone Miner Res 2001; 16: 1486-1495.

[24] Fenton TR and Gout IT. Functions and regulation of the 70kDa ribosomal S6 kinases. Int J Biochem Cell Biol 2011; 43: 47-59.

[25] Pullen N, Dennis PB, Andjelkovic M, Dufner A, Kozma SC, Hemmings BA and Thomas G. Phosphorylation and activation of p70s6k by PDK1. Science 1998; 279: 707-710.

[26] Saitoh M, Pullen N, Brennan P, Cantrell D, Dennis PB and Thomas G. Regulation of an activated S6 kinase 1 variant reveals a novel mammalian target of rapamycin phosphorylation site. J Biol Chem 2002; 277: 20104-20112.

[27] Pearson RB, Dennis PB, Han JW, Williamson NA, Kozma SC, Wettenhall RE and Thomas G. The principal target of rapamycin-induced p70s6k inactivation is a novel phosphorylation site within a conserved hydrophobic domain. EMBO J 1995; 14: 5279-5287.

[28] Klos KS, Wyszomierski SL, Sun M, Tan M, Zhou X, Li P, Yang W, Yin G, Hittelman WN and Yu D. ErbB2 increases vascular endothelial growth factor protein synthesis via activation of mammalian target of rapamycin/p70S6K leading to increased angiogenesis and spontaneous metastasis of human breast cancer cells. Cancer Res 2006; 66: 2028-2037.

[29] Akar U, Ozpolat B, Mehta K, Lopez-Berestein G, Zhang D, Ueno NT, Hortobagyi GN and Arun B. Targeting p70S6K prevented lung metastasis in a breast cancer xenograft model. Mol Cancer Ther 2010; 9: 1180-1187.

[30] Khotskaya YB, Beck BH, Hurst DR, Han Z, Xia W, Hung MC and Welch DR. Expression of metastasis suppressor BRMS1 in breast cancer cells results in a marked delay in cellular adhesion to matrix. Mol Carcinog 2013; [Epub ahead of print].

[31] Debnath J and Brugge JS. Modelling glandular epithelial cancers in three-dimensional cultures. Nat Rev Cancer 2005; 5: 675-688.

[32] Debnath J, Muthuswamy SK and Brugge JS. Morphogenesis and oncogenesis of MCF-10A mammary epithelial acini grown in three-dimensional basement membrane cultures. Methods 2003; 30: 256-268.

[33] Price JE, Polyzos A, Zhang RD and Daniels LM. Tumorigenicity and metastasis of human breast carcinoma cell lines in nude mice. Cancer Res 1990; 50: 717-721.

[34] Zhang RD, Fidler IJ and Price JE. Relative malignant potential of human breast carcinoma cell lines established from pleural effusions and a brain metastasis. Invasion Metastasis 1991; 11: 204-215.

[35] Minn AJ, Gupta GP, Siegel PM, Bos PD, Shu W, Giri DD, Viale A, Olshen AB, Gerald WL and Massague J. Genes that mediate breast cancer metastasis to lung. Nature 2005; 436: 518-524.

[36] Zhang XH, Wang Q, Gerald W, Hudis CA, Norton L, Smid M, Foekens JA and Massague J. Latent bone metastasis in breast cancer tied to Src-dependent survival signals. Cancer Cell 2009; 16: 67-78.

[37] Zhou H and Huang S. Role of mTOR signaling in tumor cell motility, invasion and metastasis. Curr Protein Pept Sci 2011; 12: 30-42.

[38] Botteri E, Disalvatore D, Curigliano G, Brollo J, Bagnardi V, Viale G, Orsi F, Goldhirsch A and Rotmensz N. Biopsy of liver metastasis for women with breast cancer: impact on survival. Breast 2012; 21: 284-288.

[39] Steeg PS. Perspective: The right trials. Nature 2012; 485: S58-59.

[40] Marino N, Woditschka S, Reed LT, Nakayama J, Mayer M, Wetzel M and Steeg PS. Breast Cancer Metastasis: Issues for the Personalization of Its Prevention and Treatment. Am J Pathol 2013;

[41] Campbell JP, Merkel AR, Masood-Campbell SK, Elefteriou F and Sterling JA. Models of bone metastasis. J Vis Exp 2012; e4260.

[42] Xia TS, Wang GZ, Ding Q, Liu XA, Zhou WB, Zhang YF, Zha XM, Du Q, Ni XJ, Wang J, Miao SY and Wang S. Bone metastasis in a novel breast cancer mouse model containing human breast and human bone. Breast Cancer Res Treat 2012; 132: 471-486.

[43] Yang W, Lam P, Kitching R, Kahn HJ, Yee A, Aubin JE and Seth A. Breast cancer metastasis in

a human bone NOD/SCID mouse model. Cancer Biol Ther 2007; 6: 1289-1294.
[44] Iorns E, Drews-Elger K, Ward TM, Dean S, Clarke J, Berry D, El Ashry D and Lippman M. A new mouse model for the study of human breast cancer metastasis. PLoS One 2012; 7: e47995.
[45] Smid M, Wang Y, Klijn JG, Sieuwerts AM, Zhang Y, Atkins D, Martens JW and Foekens JA. Genes associated with breast cancer metastatic to bone. J Clin Oncol 2006; 24: 2261-2267.
[46] Paik S, Shak S, Tang G, Kim C, Baker J, Cronin M, Baehner FL, Walker MG, Watson D, Park T, Hiller W, Fisher ER, Wickerham DL, Bryant J and Wolmark N. A multigene assay to predict recurrence of tamoxifen-treated, node-negative breast cancer. N Engl J Med 2004; 351: 2817-2826.
[47] Klein A, Olendrowitz C, Schmutzler R, Hampl J, Schlag PM, Maass N, Arnold N, Wessel R, Ramser J, Meindl A, Scherneck S and Seitz S. Identification of brain- and bone-specific breast cancer metastasis genes. Cancer Lett 2009; 276: 212-220.
[48] Herold CI, Chadaram V, Peterson BL, Marcom PK, Hopkins J, Kimmick GG, Favaro J, Hamilton E, Welch RA, Bacus S and Blackwell KL. Phase II trial of dasatinib in patients with metastatic breast cancer using real-time pharmacodynamic tissue biomarkers of Src inhibition to escalate dosing. Clin Cancer Res 2011; 17: 6061-6070.
[49] Campone M, Bondarenko I, Brincat S, Hotko Y, Munster PN, Chmielowska E, Fumoleau P, Ward R, Bardy-Bouxin N, Leip E, Turnbull K, Zacharchuk C and Epstein RJ. Phase II study of single-agent bosutinib, a Src/Abl tyrosine kinase inhibitor, in patients with locally advanced or metastatic breast cancer pretreated with chemotherapy. Ann Oncol 2012; 23: 610-617.
[50] Maruani DM, Spiegel TN, Harris EN, Shachter AS, Unger HA, Herrero-Gonzalez S and Holz MK. Estrogenic regulation of S6K1 expression creates a positive regulatory loop in control of breast cancer cell proliferation. Oncogene 2012; 31: 5073-5080.
[51] Sinclair CS, Rowley M, Naderi A and Couch FJ. The 17q23 amplicon and breast cancer. Breast Cancer Res Treat 2003; 78: 313-322.
[52] Segatto I, Berton S, Sonego M, Massarut S, D'Andrea S, Perin T, Fabris L, Armenia J, Rampioni G, Lovisa S, Schiappacassi M, Colombatti A, Bristow RG, Vecchione A, Baldassarre G and Belletti B. Inhibition of breast cancer local relapse by targeting p70S6 kinase activity. J Mol Cell Biol 2013; 5: 428-31.
[53] Perez-Tenorio G, Karlsson E, Waltersson MA, Olsson B, Holmlund B, Nordenskjold B, Fornander T, Skoog L and Stal O. Clinical potential of the mTOR targets S6K1 and S6K2 in breast cancer. Breast Cancer Res Treat 2011; 128: 713-723.
[54] Berven LA, Willard FS and Crouch MF. Role of the p70(S6K) pathway in regulating the actin cytoskeleton and cell migration. Exp Cell Res 2004; 296: 183-195.
[55] Zhou HY and Wong AS. Activation of p70S6K induces expression of matrix metalloproteinase 9 associated with hepatocyte growth factor-mediated invasion in human ovarian cancer cells. Endocrinology 2006; 147: 2557-2566.
[56] Liu L, Li F, Cardelli JA, Martin KA, Blenis J and Huang S. Rapamycin inhibits cell motility by suppression of mTOR-mediated S6K1 and 4E-BP1 pathways. Oncogene 2006; 25: 7029-7040.
[57] Gattelli A, Nalvarte I, Boulay A, Roloff TC, Schreiber M, Carragher N, Macleod KK, Schlederer M, Lienhard S, Kenner L, Torres-Arzayus MI and Hynes NE. Ret inhibition decreases growth and metastatic potential of estrogen receptor positive breast cancer cells. EMBO Mol Med 2013; 5: 1335-1350.
[58] Foley J, Nickerson NK, Nam S, Allen KT, Gilmore JL, Nephew KP and Riese DJ 2nd. EGFR signaling in breast cancer: bad to the bone. Semin Cell Dev Biol 2010; 21: 951-960.
[59] Nie F, Yang J, Wen S, An YL, Ding J, Ju SH, Zhao Z, Chen HJ, Peng XG, Wong ST, Zhao H and Teng GJ. Involvement of epidermal growth factor receptor overexpression in the promotion of breast cancer brain metastasis. Cancer 2012; 118: 5198-5209.
[60] Lemmon MA and Schlessinger J. Cell signaling by receptor tyrosine kinases. Cell 2010; 141: 1117-1134.
[61] Mulligan LM. RET revisited: expanding the oncogenic portfolio. Nat Rev Cancer 2014; 14: 173-186.
[62] Berrada N, Delaloge S and Andre F. Treatment of triple-negative metastatic breast cancer: toward individualized targeted treatments or chemosensitization? Ann Oncol 2010; 21 Suppl 7: vii30-35.
[63] Wander SA, Zhao DK, Besser AH, Hong F, Wei JQ, Ince TA, Milikowski C, Bishopric NH, Minn AJ, Creighton CJ and Slingerland JM. PI3K/mTOR inhibition can impair tumor invasion and metastasis in vivo despite a lack of antiproliferative action in vitro: implications for targeted therapy. Breast Cancer Res Treat 2013; 138: 369-381.
[64] Mina L, Krop I, Zon RT, Isakoff SJ, Schneider CJ, Yu M, Johnson C, Vaughn LG, Wang Y, Hristova-Kazmierski M, Shonukan OO, Sledge GW and Miller KD. A phase II study of oral enza-

staurin in patients with metastatic breast cancer previously treated with an anthracycline and a taxane containing regimen. Invest New Drugs 2009; 27: 565-570.

[65] Baselga J, Semiglazov V, van Dam P, Manikhas A, Bellet M, Mayordomo J, Campone M, Kubista E, Greil R, Bianchi G, Steinseifer J, Molloy B, Tokaji E, Gardner H, Phillips P, Stumm M, Lane HA, Dixon JM, Jonat W and Rugo HS. Phase II randomized study of neoadjuvant everolimus plus letrozole compared with placebo plus letrozole in patients with estrogen receptor-positive breast cancer. J Clin Oncol 2009; 27: 2630-2637.

[66] Wolff AC, Lazar AA, Bondarenko I, Garin AM, Brincat S, Chow L, Sun Y, Neskovic-Konstantinovic Z, Guimaraes RC, Fumoleau P, Chan A, Hachemi S, Strahs A, Cincotta M, Berkenblit A, Krygowski M, Kang LL, Moore L and Hayes DF. Randomized phase III placebo-controlled trial of letrozole plus oral temsirolimus as first-line endocrine therapy in postmenopausal women with locally advanced or metastatic breast cancer. J Clin Oncol 2013; 31: 195-202.

[67] Hollebecque A, Houede N, Cohen EE, Massard C, Italiano A, Westwood P, Bumgardner W, Miller J, Brail LH, Benhadji KA and Soria JC. A phase Ib trial of LY2584702 tosylate, a p70 S6 inhibitor, in combination with erlotinib or everolimus in patients with solid tumours. Eur J Cancer 2014; 50: 876-884.